Biomass and Bioenergy 195 (2025) 107706

Contents lists available at ScienceDirect

Biomass and Bioenergy

journal homepage: www.elsevier.com/locate/biombioe

Utilizing different food cultures for wastewater treatment and enhanced power generation in microbial fuel cells

Tariq Nawaz Chaudhary [a,b], Shaheryar Ahmed [b], Muhammad Usman [b], Ali O.M. Maka [c], Shafqat Rasool [a], Mohammad Ghaleeh [a], Baixin Chen [d,*]

[a] Faculty of Arts Science and Technology, University of Northampton, United Kingdom
[b] Department of Mechanical Engineering, University of Engineering and Technology, Lahore, Pakistan
[c] The Libyan Centre for Research and Development of Saharian Communities, Murzuq, Libya
[d] School of Engineering and Physical Sciences, Heriot-Watt University, Edinburgh, United Kingdom

ARTICLE INFO

Keywords:
Microbial fuel cell
Wastewater
Food cultures
Composite anode
Power generation
Reactor optimization

ABSTRACT

This study investigates the impact of reactor architecture and biocompatibility of anode material on wastewater treatment and power generation in single-chamber (SC) and dual-chamber (DC) microbial fuel cells (MFCs) by utilizing different bacterial food cultures. Comparison between graphite-coated Cu (composite) and 304L stainless steel (SS) anodes is presented under optimized pH (7.13) and temperature (34 °C). Food cultures, especially buttermilk with an acetic acid substrate, significantly enhanced power density (PD), achieving 2.17 W/m^2 using composite anode and 1.67 W/m^2 using SS in SCMFCs. Mixed food cultures raised performance by ~50 % achieving 3.31 W/m^2 and 2.97 W/m^2 using composite and SS anodes respectively. High chemical oxygen demand (COD) removal rates (>68 %) confirm effective wastewater treatment. These findings suggest that macroporous composite anodes can improve microbial compatibility and power output in MFCs, with optimal performance observed at neutral pH and ambient temperatures.

1. Introduction

Microbial fuel cells (MFCs) are bioelectrochemical devices that treat wastewater and generate green electricity via anaerobic oxidation of organic substrates. Exoelectrogenic bacteria on the anode decompose organics, generating electrons that flow to the cathode, completing the circuit through oxygen reduction. Enhancing PD cost-effectively in MFCs requires optimized bioanode materials and configurations [1,2].

Optimizing reactor design (electrode size, spacing, and surface area), solution chemistry (conductivity, buffer capacity, pH, and temperature), and electrode performance is crucial to maximizing MFC power output [3]. While chemical catalysts like ferricyanide enhance cell potential [4], the high cost of cathode materials limits MFC commercialization [5]. Research now emphasizes advanced anode materials, as they critically influence extracellular electron transfer (EET), bacterial adhesion, substrate degradation, and biofilm formation [6,7]. Despite these advancements, the high cost and availability of suitable anode materials remain barriers to widespread MFC adoption [8].

Anode materials in MFCs have commonly included carbon-based, metal/metal oxide, and conductive polymer composites [9]. Precious metals like gold, prized for high conductivity, were initially popular, while transitional metals (copper, nickel, titanium, aluminum and stainless steel) offered cost savings but showed corrosion and expense issues [10,11]. Traditional carbon materials, though economical, suffer from low conductivity [12], requiring surface modifications such as such as heating [13], nitric acid activation [14], acid soaking [15], and ammonia treatments [16] to improve efficiency. Aziz et al. reported that N-doped reduced graphene oxide (rGO)-modified carbon aerogels from paper waste achieved a PD of 1.468 W/m^2, showing cost-effective improvements for carbon-based anodes [17]. Wang et al. demonstrated a PD of 4.99 W/m^2 with carbon foam from corncobs [18], though toxicity concerns arose later [19]. Creating porous, biocompatible, and durable anodes supports biofilm growth and boosts current density (J) [20]. Biomass-derived materials show promise in overcoming anode challenges, while metal oxide composites may address limitations but depend on cost and availability. Copper, known for high conductivity and durability, corrodes in MFCs, as Logan found with pure copper anodes. Graphene offers corrosion resistance, but it is costly. Graphite

* Corresponding author.
E-mail address: B.chen@hw.ac.uk (B. Chen).

https://doi.org/10.1016/j.biombioe.2025.107706
Received 18 December 2024; Received in revised form 31 January 2025; Accepted 8 February 2025
Available online 17 February 2025

coatings can make copper more biocompatible, minimizing corrosion and enabling its use as an anode after surface modification [21–23].

To reduce ohmic resistance for high power output, electrodes must be positioned close, with separators like anion exchange membranes (AEMs) to prevent short circuits. Multiple cathodes in SCMFCs can also enhance the performance [24]. AEMs, superior for hydroxide ion transport, enhance MFC performance [25,26]. Food processing wastewater, rich in organics, serves as an effective substrate. Genera such as Geobacter and Pseudomonas [27], along with bacteria like Acidobacteria and Proteobacteria, are electricity producers in MFCs [28]. Studies have utilized composite food waste [29], sewage sludge, and cattle dung [30]. Following this approach, Mohan et al. explored power generation using composite vegetable waste [31], while various high-fat, high-COD food cultures and wastewaters also show promise as substrates.

Globally, 1.3 billion tons of food waste contain significant organic content [32], yet traditional aerobic treatment methods face high costs and disposal issues [33]. MFCs offer a green alternative by degrading organic matter in various wastewaters, including dairy and food industry byproducts [34]. Reactor parameters—such as electrolyte temperature and pH [35], solution conductivity [36], membrane type and electrode distance [37], and electrode porosity influence MFC performance, and their optimization can boost power density. This study explores bioelectricity generation using different food cultures in three MFC models. Single-chamber MFCs (SCMFCs) with single- and double-sided air cathodes (SSAC, DSAC) were compared to dual-chamber MFCs (DCMFCs), focusing on increased cathodic surface area. Graphite-coated Cu anodes, offering biocompatibility and conductivity, were tested against stainless steel, while AEMs enabled effective hydroxide ion transport. Optimization of cathode area and AEM placement further enhanced ion transfer and power output.

2. Materials and methods

This section covers material collection, substrate formation, electrochemical measurements, membrane hot pressing, electrode formation, porosity measurements, reactor construction, and the fundamental operations of MFCs.

2.1. Food cultures

The food cultures refer to bacterial cultures derived from dietary refuse in restaurant and household wastewater. Substrates include composite food waste, buttermilk, yogurt, potatoes, rice water, molasses, yeast, and methanol-fed wastewater. Buttermilk was prepared by heating whole milk to 200 °C in a steel jar, stirred to prevent scorching, and fermented with lemon juice in a warm environment (40–45 °C). Yogurt was made by boiling whole milk above 200 °C, cooling it, adding a tablespoon of yogurt, and fermenting for 12 h before blending with water. These cultures, containing lactic acid bacteria (e.g., Lactobacillus and Streptococcus), enhance microbial diversity and promote electron transfer in microbial fuel cells (MFCs). Potato culture was made by shredding leftover peels and mixing with distilled water, with large particles filtered out. A 7-liter potato paste was divided into seven cells with varying pH and electrode materials. Rice was boiled to a paste, cooled, mixed with glucose, and filtered. Yeast and methanol were purchased and prepared with water, then filtered. Various concentrations were tested for pH, electrical conductivity, and chemical properties before and after operation.

A mixed food culture was created by enriching sewage wastewater with designed synthetic wastewater (DSWW) and adding food cultures to enhance organic content. Acetic acid and phosphate buffer adjusted the pH of high COD samples. The mixtures were monitored under various pH and temperature conditions.

2.2. Electrodes formation

In this study, fine meshes of Cu, Zn, and stainless steel were utilized, specifically 304-L stainless steel mesh (SSM) with a pore size of approximately 0.3 mm and a wire diameter of 0.10 mm, serving as anodes and cathodes in dual-chamber microbial fuel cells (DCMFCs). The SSM electrodes underwent surface treatment in a 10 M HCl solution for 12 h to remove oxides and were subsequently immersed in ethanol. After being cut into pieces, they were cleaned by dipping in ethanol and boiling water above 100 °C for 6–7 min, then dried with an air blower. Two identical SSM pieces were folded into a long rectangular strip to enhance biofilm formation. Pure Cu meshes and Zn strips were only cleaned with ethanol. The Cu meshes, which offer good electrical conductivity but lack biocompatibility, were first cleaned with 10 % HCl to eliminate the oxide layer and then coated with a conductive paste made of 70 % graphite powder and 30 % acrylic glaze. This mixture was applied to the macroporous Cu meshes, which were kept in a heated airtight container to ensure a strong coating. The Zn cathodes were prepared in rectangular plates (1 mm thick, 88.9 mm × 88.9 mm) and tested alongside SSM and Cu in various configurations within the microbial fuel cells. Effective porosity of the electrodes was measured using the liquid displacement method, where the change in water volume before and after submerging the porous meshes indicated the void volume, allowing the calculation of porosity ratios and is given by.

$$\Phi\,(\%) = \frac{V_V}{V_T} \times 100 \tag{1}$$

where V_V represents the void volume, V_T represents the total volume of liquid. The porosity of the meshes was measured using the liquid displacement method before and after surface modifications. The porosity values obtained were 42 % for the composite anode, 47 % for the 304-L stainless steel anode, and 37 % for the Zn anode used in DCMFCs with the measured surface area of ~9.58 cm^2 set for each of these porous electrodes.

2.3. Membrane formation

An AEM with an exchange capacity of 1.1 mmol g^{-1} was used. For dual-chamber microbial fuel cells (DC MFCs), the AEM was cut into a circular shape and tightly pressed between the tubes of both compartments. In single-chamber microbial fuel cells (SCMFCs), the membranes were cut into 88.9 mm × 88.9 mm pieces and hot pressed against the air-side Zn cathodes, securely fastening them to the cathodic face.

2.4. Design, construction, and operation

2.4.1. DCMFCs construction and operation

A 3D model of U-Tube (UT) glass chambers was created in SOLIDWORKS and fabricated. A rubber seal was installed at the top arm of the anode compartment to maintain an anaerobic environment. Two identical dual-chamber microbial fuel cells (DCMFCs) were constructed using cylindrical glass tubes measuring 35 cm in length, 7 cm in outer diameter, and 6.03 cm in inlet diameter, with a total volume of 1000 ml and a working volume of 500 ml per chamber. The inlet tube had a diameter of 3 cm, and the anodic chamber featured an additional tubular arm with a 1 cm internal diameter and 5 cm length. Circular holes of 1 cm diameter were made in the cathodic chamber to facilitate continuous oxygen supply from ambient air. Each chamber included a tubular path at the bottom for a permeable ion exchange membrane, and the inlet of the anodic chamber was sealed with rubber corks to allow circuit wires. Porous electrodes connected to the circuit wires were placed inside the chambers, with Cu mesh used as the anode and Zn as the cathode in the first cell, while SS mesh served as the anode in the second cell. The macroporous stainless steel, Cu, and Zn meshes were folded into rectangular plates measuring 10 cm × 2 cm and immersed in substrates for

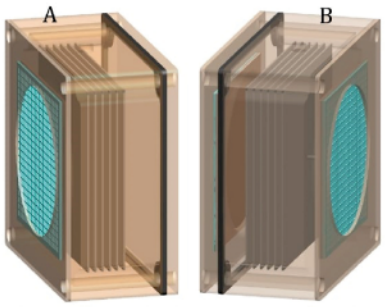

A: Single chamber microbial fuel cells (SCMFCs) with single sided air cathodes (SSAC)
B: Single chamber microbial fuel cells (SCMFCs) with Double sided air cathodes (DSAC)

Item no.	Part	Description	Quantity
1	Anode	Macro porous graphite coated Cu/SS composite anode	2
2	Cathode	Flat plate Zn Air-cathode	3
3	Cathode Gasket	Soft rubber provided between cathode and spacers for air tightness	3
4	Gasket	Soft rubber provided between chamber and endplate for air tightness	2
5	AEM	Anion exchange membrane for selective Hydroxide Ions Transport	3
6	Anodic Chamber	Reaction Chamber with inlet and outlet holes for anolyte	2
7	Cathode Endplate	Air sided cathode endplate for tightness	3
8	Spacer	Mesh Spacers	9
9	Grooved Plate	Additional plate for reactor modification and providing DSAC	1
10	Anode Endplate	Opposite face extruded plate for perfect air tightness	1

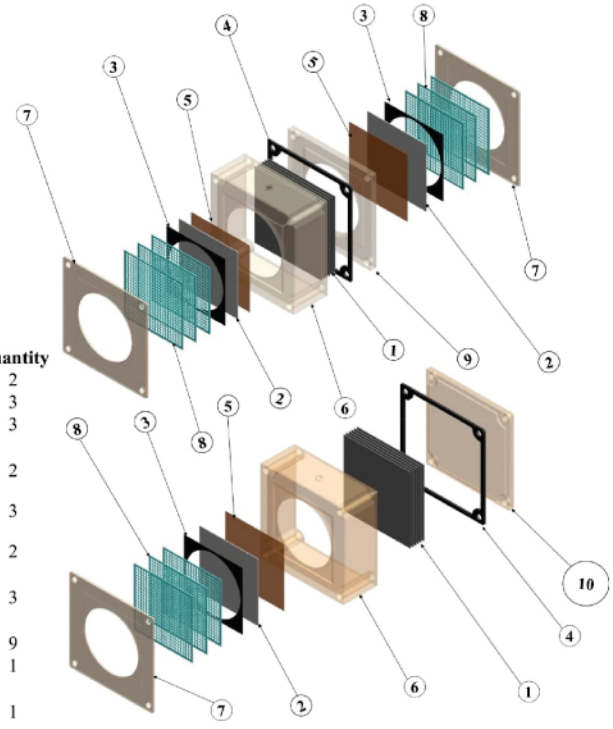

Fig. 1. Exploded view of two reactor modules with assembly and bill of material (BOM).

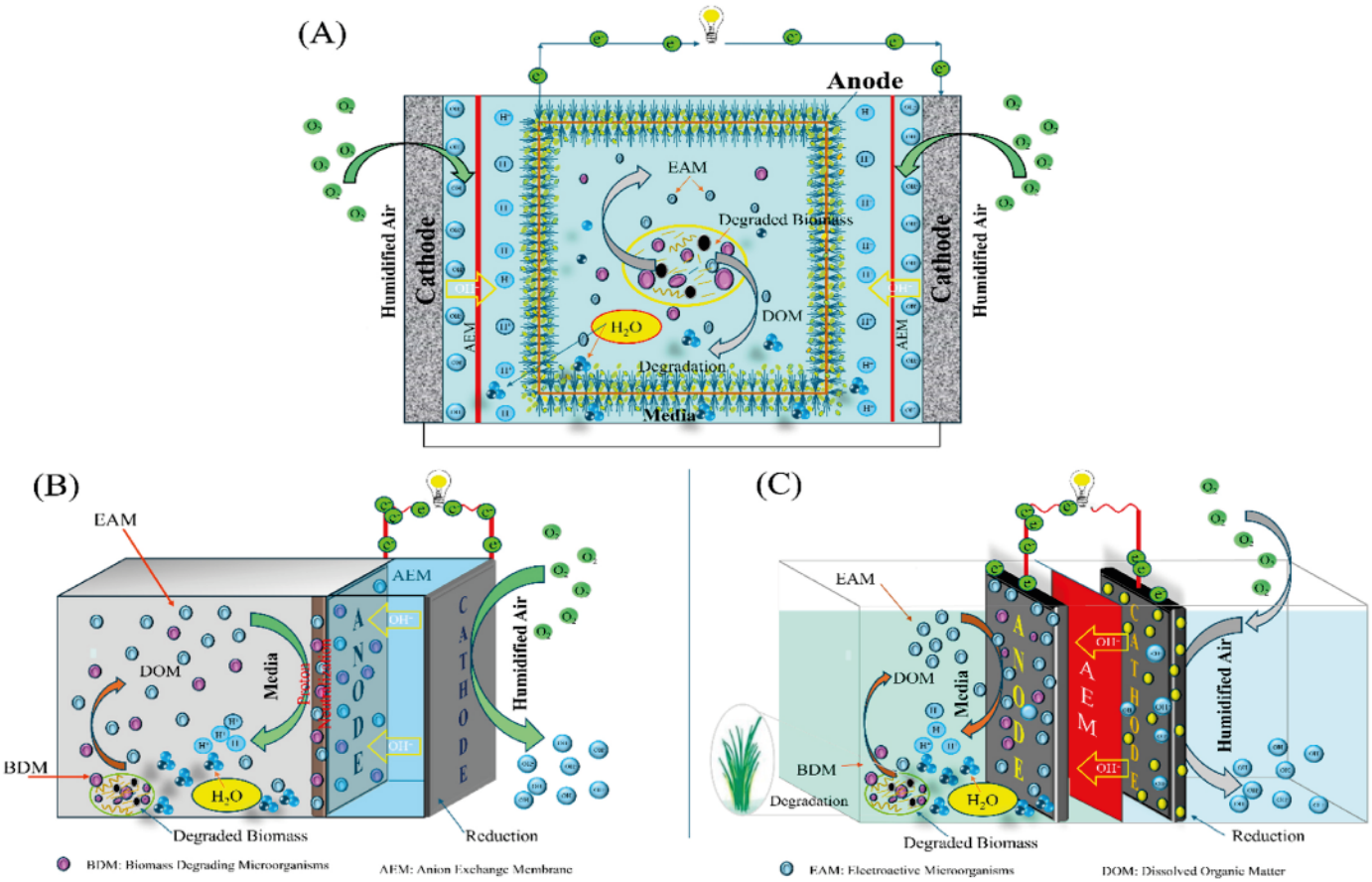

Fig. 2. Schematic of three reactor types with AEM: (A) SCMFC with DSAC, (B) SCMFC with SSAC, and (C) DC-MFC operation.

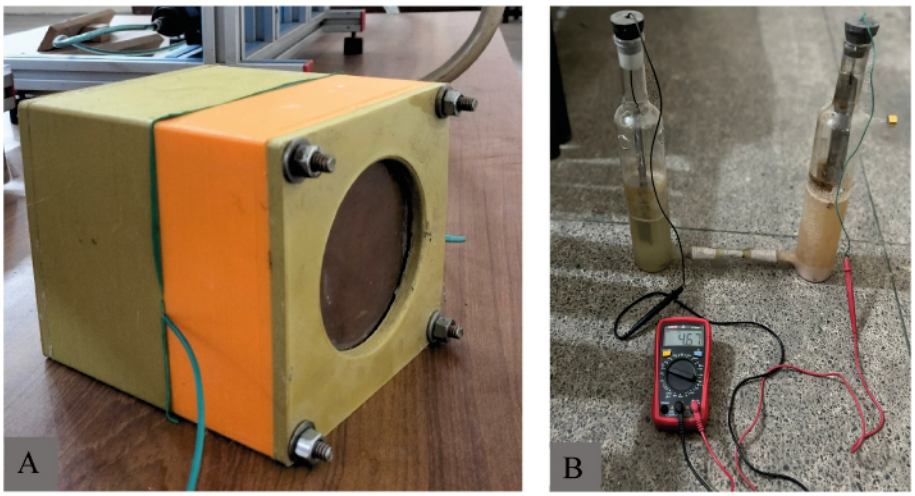

Fig. 3. Physical prototypes of MFCs: (A) large DSAC SCMFC and (B) U-Tube DCMFC.

operation, separated by an AEM with an area of 0.7853 cm^2.

2.4.2. Air cathode SCMFCs construction and operation

A closely spaced air cathode single-chamber microbial fuel cell (SCMFC) model (V = 127 mm × 127 mm × 63.5 mm) with a 6.35 mm wall thickness designed and 3D printed after slicing using Prusa Slicer as shown in Fig. 1. An anodic cover supported to ensure airtight chambers and flat square plates (A = 127 mm × 127 mm) with 76.2 mm circular holes to support air cathodes. The chamber was sealed after inserting the anode electrode. Fig. 1 shows the exploded view of two different models of SCMFCs.

Acetic acid and phosphate buffer were added to optimize conditions for microbial activity and electron transfer. Food cultures were introduced sequentially into the anodic chamber of dual-chamber microbial fuel cells (DCMFCs) using graphite-coated Cu anodes and Zn cathodes. Each reaction lasted five days, with acetic acid and phosphate buffer added to maintain stable pH and temperature for enhanced biofilm growth.

Fig. 2 shows electronic images of SC-MFC (A) with DSAC (B) with SSAC and (C) DCMFCs which describe the whole operation pictorially. A physical prototype is shown in Fig. 3. The environmental conditions maintained at 32, 34, 36 °C marked as slightly lower, room, and slightly higher temperatures respectively, with pH adjusted through buffer solution. In DCMFCs, organic matter oxidation produced H^+ ions in the anolyte, while reduction in the cathodic chamber generated OH^- using humidified air. SCMFCs operated without a catholyte, pressing AEMs against air cathodes for anaerobic oxidation. Overall, both reactor types were analyzed under optimized pH (7.13) and temperature (34 °C) conditions, with general half-cell reaction equations used for acetic acid substrates.

A similar methodology was applied to SCMFCs with DSACs, enhancing electricity generation due to oxidation occurring at both ends facing the air-side cathodes. The generated OH^- ions move through the AEMs, neutralizing H^+ ions in the anolyte to form water. The basic reactions involving acetic acid substrates are represented by the following equations.

$$CH_3COOH + H_2O \rightarrow 2CO_2 + 8H^+ + 8e- \quad (2)$$

$$O_2 + 4e- + 4H^+ \rightarrow 2H_2O \quad (3)$$

Experiments were conducted using composite food waste and individual substrates, including buttermilk, yogurt, potato, rice water, molasses, methanol, and yeast wastewater. Acetic acid was added every 30 min to enhance bacterial biofilm thickness. Treated wastewater samples were analyzed for COD removal efficiency using the closed reflux titrimetric method. Key parameters such as anode porosity, electrode sizes, active areas, membrane area, solution chemistry (conductivity and buffer capacity), temperature, and pH were evaluated to improve the productivity of the microbial fuel cells (MFCs).

Table 1
Preliminary chemical characteristics of influents acquired after mastication and separation via fluted filter paper.

NO.	Cultures	Initial Chemical Properties		
		pH	EC (mS/cm)	Initial COD (mg/L)
1.	Mixed food	9.32	27.64	29000
2.	Buttermilk	6.17	15.59	18900
3.	Yogurt	9.85	15.40	18200
4.	Potato	9.72	16.65	23000
5.	Rice Water	6.91	18.02	10200
6.	Molasses	6.89	17.21	10000
7.	Methanol	7.64	7.38	7670
8.	Yeast	6.12	7.27	7800

2.5. Measurement of electrochemical properties

The electrochemical properties of influents and effluents were measured, as shown in Table 1. For pH and conductivity analysis, 100 ml samples were taken in glass beakers, using a pH meter and conductometer. COD was measured with a closed reflux titrimetric method: 20 ml of culture wastewater was refluxed in 30 ml of 98 % sulfuric acid with 0.025 N potassium dichromate, silver sulfate, and mercuric sulfate at 90 °C for 2 h [38]. After digestion, the remaining dichromate was titrated with 0.025 N ferrous ammonium sulfate, using ferroin as an indicator. COD was calculated based on Equation (4).

$$COD\ \frac{mg}{L} = (\alpha - \beta)\eta \times \frac{8000}{mL\ of\ Sample} \quad (4)$$

Where α represents the volume of ferrous ammonium sulfate solution required for titration of blank, β is the volume of ferrous ammonium sulfate solution required for titration of blank, and η is the normality of ferrous ammonium sulfate solution.

An external resistance of 10Ω was connected to the voltage (V) values measured using a digital multimeter. Ohm's law (I = V/R) and the power formula (P = V/I) were applied to calculate the current (I) and power (P). The current and power were then normalized by the electroactive surface area of the anode (~9.58 cm^2) to determine the current density (J = I/As) and power density (PD = P/As). Polarization tests were conducted for three different configurations using external

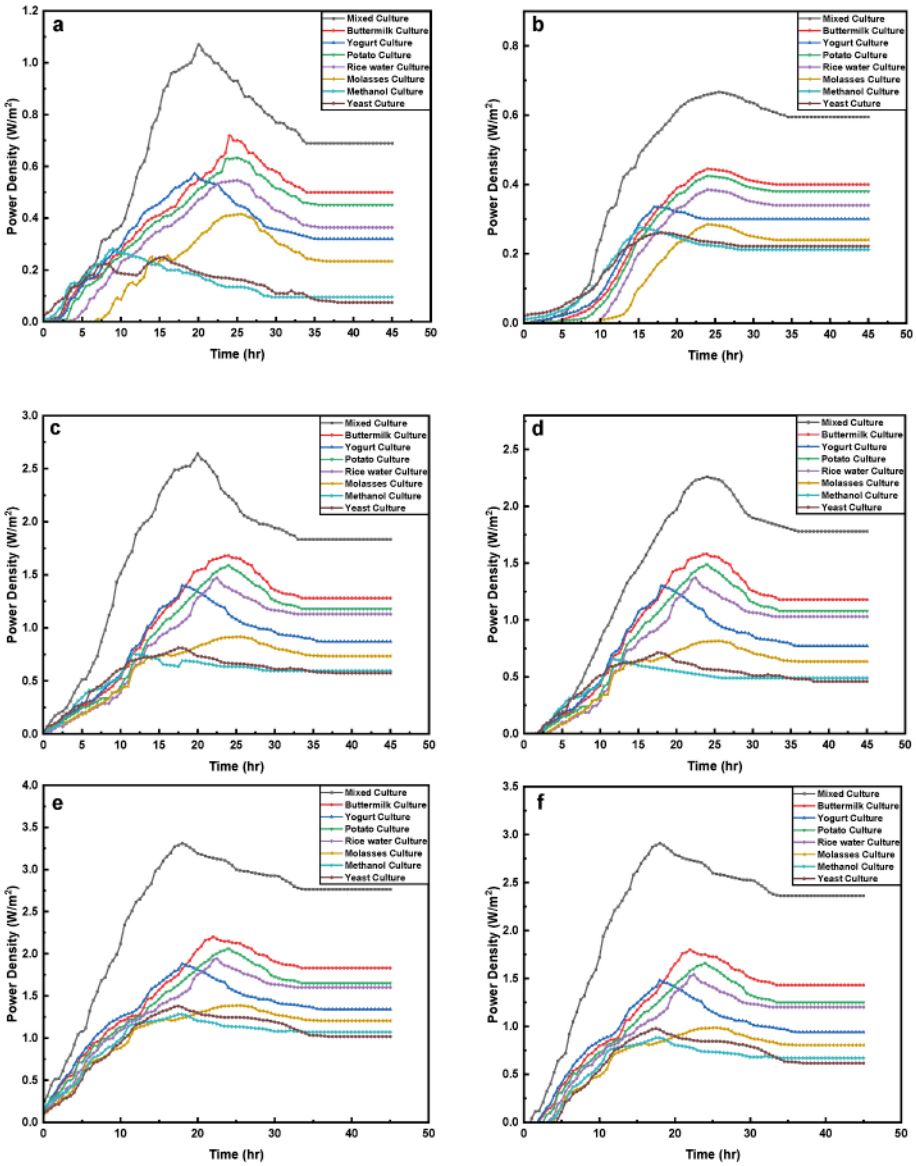

Fig. 4. MPD curves showing the effect of reactor architecture and food cultures: (a, c, e) using composite anode and (b, d, f) using SS anode. Sub-Figs (a, b), (c, d), and (e, f) display outputs from DCMFCs, SCMFCs with SSAC, and SCMFCs with DSAC, respectively.

resistances of 1000, 500, 200, 100, 50, 30, 20, 10, 5, and 3 Ω, with measurements taken at 20-min intervals.

3. Results and discussion

This study observed the fundamental reactions in single- and double-chamber MFCs. Macroporous Cu anodes and Zn cathodes produced maximum PD with mixed food cultures, as shown in Table 1.

3.1. Performance analysis and validation

3.1.1. Effect of reactor architecture and food cultures

Fig. 4 shows PD curves from various food cultures using composite (Fig. 4a–c, e) and SS anodes (Fig. 4b–d, f) across different reactors: DCMFCs (Fig. 4a and b), SCMFCs with SSAC (Fig. 4c and d), and SCMFCs with DSAC (4e, f). Over a three-day operation, peak PD of 1.07 W/m^2 was achieved after 20 h in DCMFCs (Fig. 4a) with acetic acid supplementation, boosting microbial activity [29]. This value is 29.8 % higher than the 0.824 W/m^2 achieved by Dessie et al. with α-MnO_2/PANI composites and 70 % higher than the 0.283 W/m^2 reported by Rahimnejad et al. [39].

Among food cultures, buttermilk reached the highest PD of 0.719 W/m^2 at 24 h, followed by potato at 0.633 W/m^2 in 25 h, yogurt at 0.572 W/m^2 in 20 h, rice water at 0.546 W/m^2 in 26 h, and molasses at 0.414 W/m^2. Buttermilk's higher lactic and acetic acid content increased conductivity (15.59 mS/cm), while potato's higher organic load enhanced its power output compared to yogurt. Din et al. also observed optimal PD with potato peel waste at neutral pH, recording 0.633 W/m^2 [35].

Glucose-rich rice water and molasses yielded lower PD than acetic-acid-rich foods. The fundamental reaction of glucose with water is represented as.

$$C_6H_{12}O_6 + 6H_2O \rightarrow 6CO_2 + 24H^+ + 24e^- \quad (5)$$

Methanol and yeast cultures showed unique behaviours, with maximum PDs of 0.281 W/m^2 at 9 h and 0.249 W/m^2 at 16 h, respectively (Fig. 4b). SS anode DCMFCs achieved peak PDs of 0.667 W/m^2 at 26 h and 0.425 W/m^2 at 24 h, confirming SS's lower conductivity relative to composite anodes. In SCMFCs, PDs of 2.64 and 3.31 W/m^2 were reached in 20 h using SSAC and DSAC setups, respectively (Fig. 4e

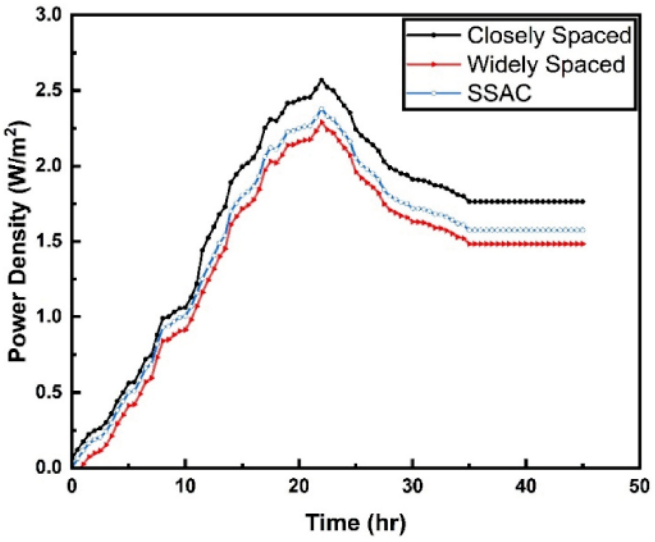

Fig. 5. PD curves obtained from large sized reactor under optimized conditions.

and f). The AEM-supported DSAC SCMFC achieved 38 % and 7 % higher PDs than MFCs with acetate and phosphate buffer solutions using UFM (2.4 W/m^2) and CEM (3.1 W/m^2) but was still 62 % lower than AEM-MFC (8.8 W/m^2). These findings indicate the importance of regular organic additions and AEM's role in efficient OH- transfer, as shown by Rossi et al. [26].

Fig. 5 shows that reactor architecture significantly impacts PD in large-sized SCMFCs. With composite food waste at neutral pH and room temperature, the increased reactor size and electrode spacing led to decreased PD, though maximum PD of 2.64 W/m^2 was achieved by reducing reactor volume and spacing in DSAC. Table 2 compares previous MFC research, with PD values ranging from 0.0022 to 4 W/m^2. In this study, PD values ranged from 0.667 to 3.31 W/m^2, aligning well with these established benchmarks.

3.1.2. Effect of pH variation

The study's results align with previous findings under varying pH conditions. The maximum PD of 3.31 W/m^2 was achieved using a composite anode in closely spaced SCMFCs with AEMs at pH 7.13 (Fig. 6a). Fig. 6(a–c, e) and (b, d, f) show PD curves from mixed food waste using composite and SS anodes, respectively, across reactors: DCMFCs (a, b), SCMFCs with SSAC (c, d), and SCMFCs with DSAC (e, f). Seven initial pH values (4, 5, 6, 7.13, 8.5, 10, 12) were tested, revealing optimal PD near neutral pH, with performance declining as pH deviated from neutral.

The study confirms that neutral pH is ideal for MFC performance, as significant pH deviation reduces PD. Alkaline environments initially increase PD but do not sustain it. Findings in Table 2 indicate the best conditions are room temperature, neutral pH, and acetic acid substrate. Previous research supports this, noting that bacterial physiology and PD in MFCs are highly pH-dependent: optimal pH ranges near 6.5–7.3 show greater PD [53–56]. Alkalization of the cathode and acidification of the anode, common in MFCs, reduce microbial activity and electron transfer, impacting PD negatively [57]. Efficient ion transfer at pH 8, promoted by acetic acid, supports microbial growth, whereas values below pH 6 or above 9 reduce current production [50]. Ren et al. reported power losses when pH dropped to 5.2 but recovery when adjusted to 7 [58], further demonstrating that a feed pH of 8.0 offers higher PD through reduced internal resistance [50].

3.1.3. Effect of temperature

The experimental results from this study indicate that power density (PD) decreases above and below room temperature (34 °C), as shown in Fig. 7(a–c, e) and Fig. 7(b–d, f). Mansoorian et al. reported a maximum PD of 0.621 W/m^2 at 35 °C [46], while Din et al. achieved maximum voltage and current (1.12 V, 12.45 mA) at room temperature and neutral pH [35]. Min et al. observed peak performance at 30 °C with 70 mW/m^2 [59]. Several studies noted a linear increase in power output from 20 °C to 35 °C [60–62], Fig. 7 illustrates the PD variations at 30 °C, 34 °C, and 38 °C under neutral pH conditions. Results are consistent with previous

Table 2
Comparison of MFC Performances with different substrates under different operating conditions.

Catalyst/Substrate	pH	COD Removal (%)	MPD (W/m^2)	Anode	Organic fuel/Culture	References
CH_3COONa	7	—	2.97	C-Brush	Nutrient carbon solution	[10]
CH_3COONa	7	~100	4.99	C-Foam	Mixed Culture	[18]
$C_6H_{12}O_6$	6.02	74.59	0.824	(α-MnO_2-Graphite)	University Effluent	[40]
CH_3COOH	10.5	88	1.043	SS fiber felt	Yogurt wastewater	[41]
		97	0.221			
$C_6H_{12}O_6$	6.5	—	0.283	Bioanode	Pure Saccharomyces cerevisiae	[39]
AC: PTFE (6:1)	8.2	—	0.426	Graphite fiber	Anaerobic sludge from PSU	[42]
CH_3COOH	9.5	—	0.833	CC	Domestic wastewater	[43]
$C_6H_{12}O_6$	10.0	81	0.213	Graphite felt	Yeast	[44]
CH_3COOH	~10.0	91	0.161	SS Mesh	Dairy wastewater	[45]
CH_3COOH	8.5–10	90	0.621	Bioanode	Industrial dairy wastewater	[46]
CH_3COOH	—	—	4.0	Platinum	Pure G. Sulfurreducens (Soil)	[47]
No	7.5	18	Negligible		Banana peel	[48]
S. Cerevisiae		44	0.0022	304 SS Mesh		
No	7.9	70	0.0446		Banana peel slurry	
S. Cerevisiae		88	0.0869			
CH_3COONa	—	92	1.06	C-Brush	Domestic Wastewater	[49]
$C_6H_{12}O_6$	6.0	47.8	0.158	SS Mesh	Synthetic wastewater	[50]
	8.0	40.4	0.600			
$C_{14}H_{26}O_{11}$	6.2	—	1.78	—	Algae	[51]
CH_3COONa	7	86.95	0.216	C-Paper	Potato Wastewater	[52]
CH_3COOH	7.13		3.31/2.91 2.64/2.26 1.07/0.667	(Composite/304L SS)	Composite Food Wastewater	Current Research

* BOM: Bacterial Outer Membrane.
* CEA: Cloth electrode assemblies.
* CC: Carbon Cloth.
* PSU: Penn State University.

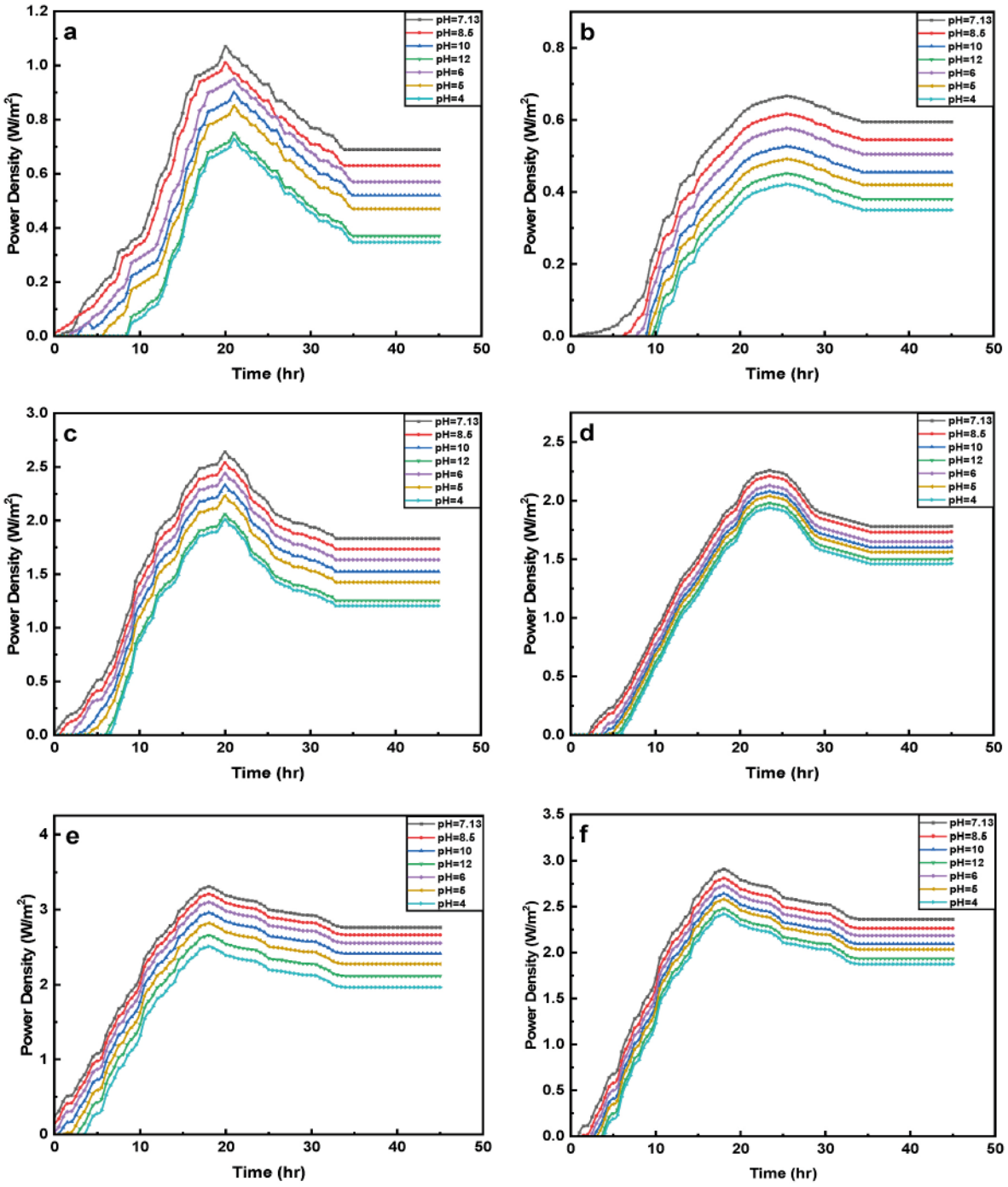

Fig. 6. Power density (PD) curves using composite food waste from various reactors under different pH conditions using composite and SS anodes: (a, c, e) for DCMFCs, SCMFC with SSAC, and SCMFC with DSAC using composite anodes; (b, d, f) for the same reactors using SS anodes.

studies, indicating optimal performance around room temperature, with decreased PD at temperatures above 38 °C [63,64]. Moon et al. found improved performance from 24 °C to 35 °C but a drop at 38 °C and 41 °C, while Li et al. observed decreased PD from 37 °C to 43 °C [66, 67]. Patil et al. also noted a decline in current density above 40 °C [63].

This study confirms that MFC performance peaks at room temperature, with all reactor configurations showing similar trends. Increased substrate oxidation rates occur until 30 °C, followed by a plateau and subsequent decline. Thus, room temperature is the ideal condition for maximizing power generation in MFCs.

3.2. Performance and stability of MFCs

The PD region provides the internal resistance. Long-term performance was monitored over five days with an external resistance of 10 Ω, which was reduced to 5 Ω for 2 h on the second day, then returned to 10 Ω. Polarization curves in Fig. 8 (A) show that DSAC-SCMFC achieved a maximum PD of 3.30 W/m^2, about 20 % higher than SSAC (2.62 W/m^2) and 68 % higher than DCMFC (1.05 W/m^2) under optimized temperature and pH conditions with mixed food culture and composite anode. Linearization of the maximum power region yielded internal resistances (Rint) of 4.41, 5.13, and 18.39 mΩ m^2 for these reactors, respectively. The very high Rint for DCMFC suggests dominant ohmic losses due to

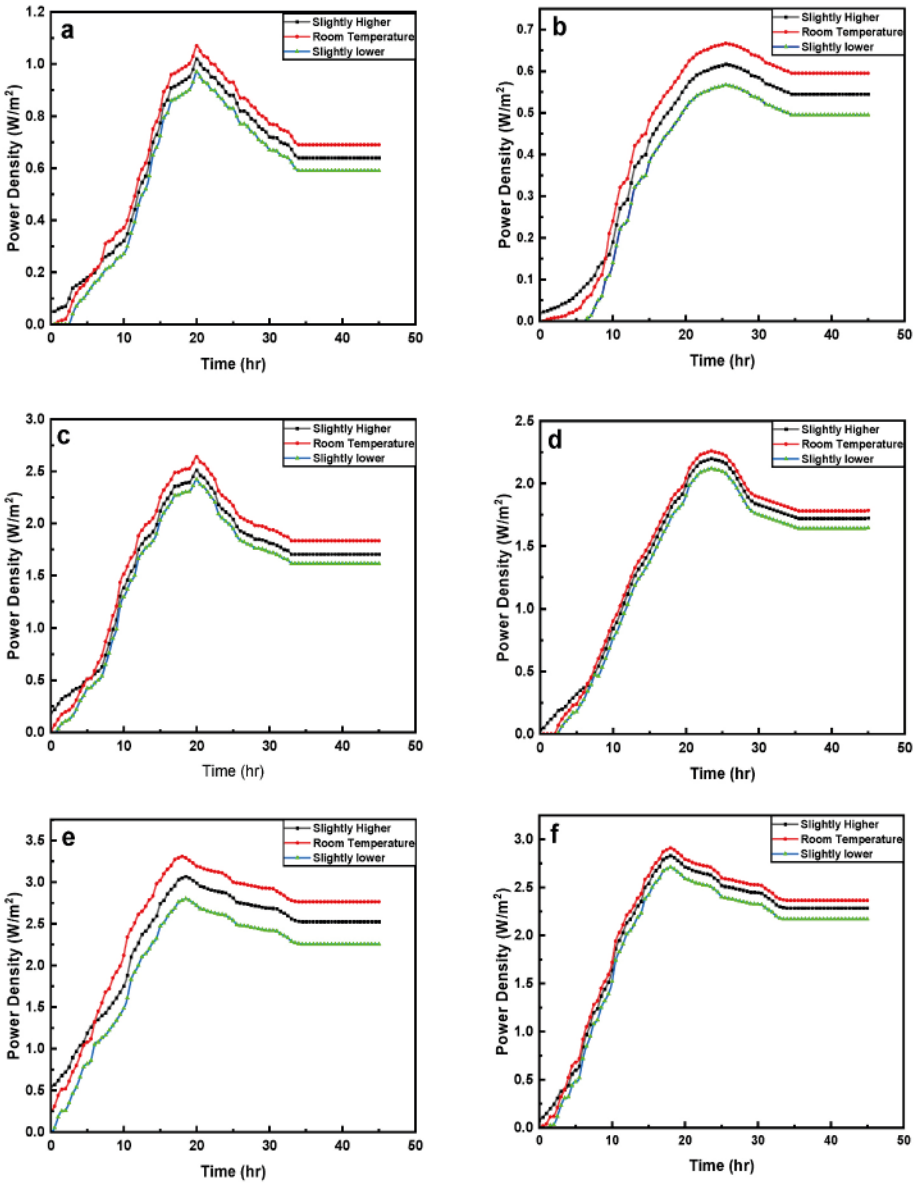

Fig. 7. PD curves at varying temperatures from different reactors using composite and SS anodes: (a, c, e) for composite anode (DCMFCs, SCMFC with SSAC, SCMFC with DSAC) and (b, d, f) for SS anode (same reactors).

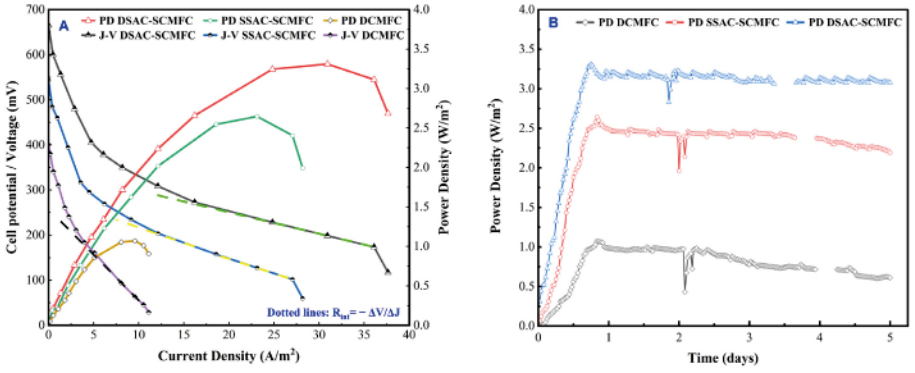

Fig. 8. (A) MFC performance for different configurations in polarization tests and (B) Long term performance.

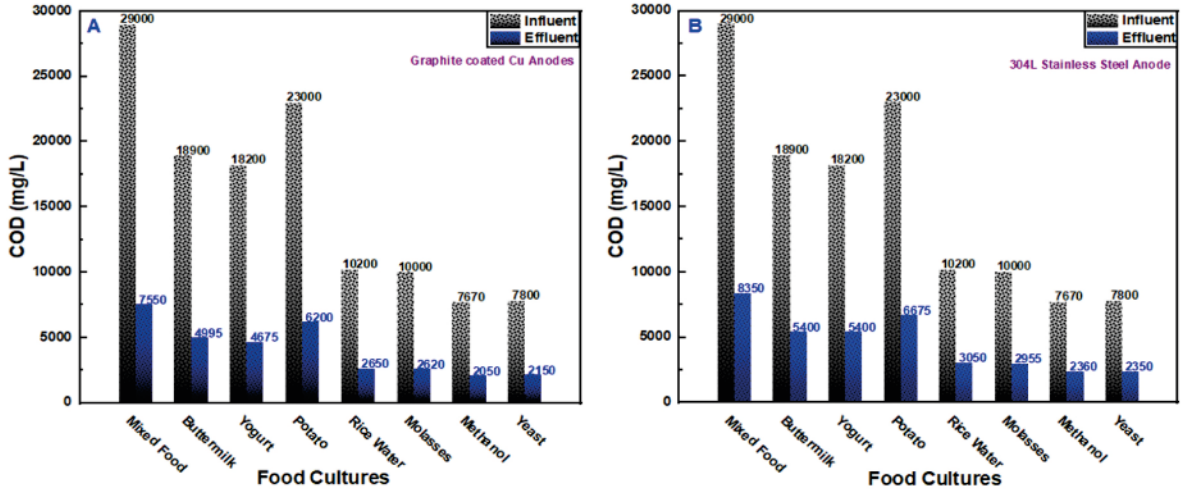

Fig. 9. COD removal in DSAC SCMFCs using (A) graphite-coated Cu anode (73 % efficiency) and (B) 304L SS anode(70 % efficiency).

the larger distance between electrodes, despite effective hydroxide ion transport through the AEM. MFCs need to maintain high power output over time without rapid decline.

Fig. 8 (B) shows that DSAC-SCMFC produced stable output over five days, peaking at 3.31 W/m^2 on day 2 (at 10 Ω), with a ~7 % drop (to 3.07 W/m^2) by day 5. The maximum PD over five days (3.31 W/m^2) with a 10 Ω external resistance was like the polarization test result (3.30 W/m^2), confirming that the test accurately reflected MFC performance during continuous operation. In comparison, SSAC-SCMFC performance dropped by ~20 % (from 2.64 to 2.19 W/m^2), and DCMFC performance dropped by ~35 % (from 1.07 to 0.609 W/m^2) over the same period, likely due to the single cathode and increased electrode distance in these reactors. Polarization tests conducted between the fourth and fifth days further indicate the performance of the MFCs and linearization in the maximum power density region.

3.3. Chemical oxygen demand (COD) REMOVAL EFFICIENCY

To evaluate MFC performance, COD is critical as it quantifies how much substrate fuel is converted into electrical current [45]. In this study, COD levels were measured before and after MFC treatment: initially, the composite food wastewater COD was 29,000 mg/L, decreasing to 15,100 mg/L post-treatment. This 40 % COD reduction demonstrates effective substrate degradation, likely due to bacterial activity that oxidizes the substrate, using carbon as an electron donor. These findings indicate MFCs can efficiently degrade organic materials, especially potato waste, at neutral pH, as calculated using Equation (6).

$$COD\ Removal\ (\%) = \frac{COD_{influent} - COD_{effluent}}{COD_{influent}} \times 100 \quad (6)$$

Fig. 9 (A) and (B) illustrate influent and effluent COD values, showing an average COD removal efficiency of 73 % and 70 % for DSAC SCMFCs. This suggests that the composite graphite-coated Cu anode enhances COD removal and biofilm formation. SCMFCs offer high COD removal efficiency with reduced sludge handling compared to traditional aerobic/anaerobic systems, which, while effective, have high operating costs and sludge disposal issues. SCMFCs, operating anaerobically at room temperature and neutral pH, achieved an average COD removal of 78 % in larger reactors, making them suitable for integrated, power-free wastewater treatment systems.

3.4. Benefits

Implementing MFCs can support sustainability goals in hotels and restaurants by reducing carbon footprints and minimizing the need for traditional, resource-heavy wastewater treatments, thus lowering chemical and energy use. Resource benefits and energy output vary by system size, wastewater type, and investment level. For hospitality businesses, assessing capital, operational costs, and return on investment (ROI) is essential to determine MFC suitability. Although MFCs show promise in sustainability, results may differ across locations. Additionally, dairy waste from restaurants, along with municipal and food processing waste, is abundant in organic content and could serve effectively as an MFC substrate.

4. Conclusion

The study demonstrated that using acetic acid substrates and porous anodes in MFCs enhances bacterial deposition, significantly boosting power density (PD). Testing different food cultures under optimized pH and temperature conditions revealed that low-cost, porous electrodes in air-cathode SCMFCs outperformed traditional DCMFCs, especially when combined with Cu/Zn electrodes. Nearly zero-gap DSAC SCMFCs with AEMs achieved maximum PD of 3.31 W/m^2 using a composite anode and Zn cathode at neutral pH and room temperature surpassing previous results with alkaline wastewater. The AEM facilitated OH^- transfer, further increasing PD. MFCs present a valuable solution for the hospitality industry, offering sustainable wastewater treatment, on-site energy generation, and reduced environmental impact. The findings also highlight MFC potential for municipal and food processing facilities, with anaerobic digestion of organic waste yielding high energy. These insights expand the application potential of MFCs under optimized conditions with larger cathodic surfaces.

CRediT authorship contribution statement

Tariq Nawaz Chaudhary: Writing – original draft, Investigation, Conceptualization. **Shaheryar Ahmed:** Validation, Software, Methodology. **Muhammad Usman:** Resources, Data curation. **Ali O.M. Maka:** Visualization. **Shafqat Rasool:** Formal analysis. **Mohammad Ghaleeh:** Project administration. **Baixin Chen:** Writing – review & editing, Supervision.

Acknowledgements

The University of Northampton, United Kingdom, and University of Engineering & Technology, Lahore, Pakistan, are highly acknowledged for providing the facilities and support for this research work.

Data availability

Data will be made available on request.

References

[1] D. Massazza, R. Parra, J.P. Busalmen, H.E. Romeo, New ceramic electrodes allow reaching the target current density in bioelectrochemical systems, Energy Environ. Sci. 8 (9) (Sep. 2015) 2707–2712, https://doi.org/10.1039/c5ee01498k.

[2] R. Rossi, B.E. Logan, Impact of External Resistance Acclimation on Charge Transfer and Diffusion Resistance in Bench-Scale Microbial Fuel Cells, 2020.

[3] S. Gadkari, J.M. Fontmorin, E. Yu, J. Sadhukhan, Influence of temperature and other system parameters on microbial fuel cell performance: numerical and experimental investigation, Chem. Eng. J. 388 (May 2020), https://doi.org/10.1016/j.cej.2020.124176.

[4] K. Lawson, R. Rossi, J.M. Regan, B.E. Logan, Impact of cathodic electron acceptor on microbial fuel cell internal resistance, Bioresour. Technol. 316 (Nov) (2020), https://doi.org/10.1016/j.biortech.2020.123919.

[5] T.H.J.A. Sleutels, A. Ter Heijne, C.J.N. Buisman, H.V.M. Hamelers, Bioelectrochemical Systems: an Outlook for Practical Applications, Wiley-VCH Verlag, 2012, https://doi.org/10.1002/cssc.201100732.

[6] A.A. Yaqoob, M.N.M. Ibrahim, C. Guerrero-Barajas, Modern Trend of Anodes in Microbial Fuel Cells (MFCs): an Overview, Elsevier B.V., Aug. 01, 2021, https://doi.org/10.1016/j.eti.2021.101579.

[7] R. Kaur, A. Marwaha, V.A. Chhabra, K.H. Kim, S.K. Tripathi, Recent Developments on Functional Nanomaterial-Based Electrodes for Microbial Fuel Cells, Elsevier Ltd., Mar. 01, 2020, https://doi.org/10.1016/j.rser.2019.109551.

[8] R. Rossi, P.J. Evans, B.E. Logan, Impact of flow recirculation and anode dimensions on performance of a large scale microbial fuel cell, J. Power Sources 412 (Feb. 2019) 294–300, https://doi.org/10.1016/j.jpowsour.2018.11.054.

[9] B. Liang, et al., Hierarchically porous N-doped carbon encapsulating CoO/MgO as superior cathode catalyst for microbial fuel cell, Chem. Eng. J. 385 (Apr) (2020), https://doi.org/10.1016/j.cej.2019.123861.

[10] Y. Wang, L. Zhu, L. An, Electricity generation and storage in microbial fuel cells with porous polypyrrole-base composite modified carbon brush anodes, Renew. Energy 162 (Dec. 2020) 2220–2226, https://doi.org/10.1016/j.renene.2020.10.032.

[11] M. Shirkosh, Y. Hojjat, M.M. Mardanpour, Boosting microfluidic microbial fuel cells performance via investigating electron transfer mechanisms, metal-based electrodes, and magnetic field effect, Sci. Rep. 12 (1) (Dec. 2022), https://doi.org/10.1038/s41598-022-11472-6.

[12] M.D. Khan, et al., Polyaniline on stainless steel fiber felt as anodes for bioelectrodegradation of acid blue 29 in microbial fuel cells, Front. Chem. Eng. 4 (Apr) (2022), https://doi.org/10.3389/fceng.2022.877255.

[13] Y. Feng, Q. Yang, X. Wang, B.E. Logan, Treatment of carbon fiber brush anodes for improving power generation in air-cathode microbial fuel cells, J. Power Sources 195 (7) (Apr. 2010) 1841–1844, https://doi.org/10.1016/j.jpowsour.2009.10.030.

[14] G.G. Kumar, V.G.S. Sarathi, K.S. Nahm, Recent Advances and Challenges in the Anode Architecture and Their Modifications for the Applications of Microbial Fuel Cells, May 05, 2013, https://doi.org/10.1016/j.bios.2012.12.048.

[15] Mustakeem, Electrode Materials for Microbial Fuel Cells: Nanomaterial Approach, SpringerOpen, Dec. 01, 2015, https://doi.org/10.1007/s40243-015-0063-8.

[16] S. Cheng, B.E. Logan, Ammonia treatment of carbon cloth anodes to enhance power generation of microbial fuel cells, Electrochem. Commun. 9 (3) (Mar. 2007) 492–496, https://doi.org/10.1016/j.elecom.2006.10.023.

[17] N. Senthilkumar, et al., Waste paper derived three-dimensional carbon aerogel integrated with ceria/nitrogen-doped reduced graphene oxide as freestanding anode for high performance and durable microbial fuel cells, Bioprocess Biosyst. Eng. 43 (1) (Jan. 2020) 97–109, https://doi.org/10.1007/s00449-019-02208-4.

[18] Y. Wang, et al., High power generation in mixed-culture microbial fuel cells with corncob-derived three-dimensional N-doped bioanodes and the impact of N dopant states, Chem. Eng. J. 399 (Nov) (2020), https://doi.org/10.1016/j.cej.2020.125848.

[19] M. Hassan, H. Olvera-Vargas, X. Zhu, B. Zhang, Y. He, Microbial electro-Fenton: an Emerging and Energy-Efficient Platform for Environmental Remediation, Elsevier B.V., Jun. 01, 2019, https://doi.org/10.1016/j.jpowsour.2019.03.112.

[20] P. Chong, B. Erable, A. Bergel, Effect of Pore Size on the Current Produced by 3-dimensional Porous Microbial Anodes: a Critical Review, vol. 2, 2019 [Online]. Available: https://www.elsevier.com/open-access/userlicense/1.0/.

[21] X. Zhu, Bruce E. Logan, Copper anode corrosion affects power generation in microbial fuel cells, J. Chem. Technol. Biotechnol. 89 (3) (2014), https://doi.org/10.1002/jctb.4156. J. Chem. Technol. Biotechnol., vol. 89.

[22] Y. Dessie, S. Tadesse, Y. Adimasu, Improving the performance of graphite anode in a Microbial Fuel Cell via PANI encapsulated α-MnO2 composite modification for efficient power generation and methyl red removal, Chem. Eng. J. Adv. 10 (March) (2022) 100283, https://doi.org/10.1016/j.ceja.2022.100283.

[23] L. Gonzalez Olias, P.J. Cameron, M. Di Lorenzo, Effect of electrode properties on the performance of a photosynthetic microbial fuel cell for atrazine detection, Front. Energy Res. 7 (Oct) (2019), https://doi.org/10.3389/fenrg.2019.00105.

[24] M. Masoudi, M. Rahimnejad, M. Mashkour, Enhancing operating capacity of microbial fuel cells by using low-cost electrodes and multi anode-cathode connections in a membrane-less configuration, Int. J. Hydrogen Energy 46 (11) (2021) 8226–8238, https://doi.org/10.1016/j.ijhydene.2020.12.019.

[25] Y. Fan, H. Hu, H. Liu, Enhanced Coulombic efficiency and power density of air-cathode microbial fuel cells with an improved cell configuration, J. Power Sources 171 (2) (Sep. 2007) 348–354, https://doi.org/10.1016/j.jpowsour.2007.06.220.

[26] R. Rossi, B.E. Logan, Using an anion exchange membrane for effective hydroxide ion transport enables high power densities in microbial fuel cells, Chem. Eng. J. 422 (Oct. 2021), https://doi.org/10.1016/j.cej.2021.130150.

[27] O.F. Vyatchina, D.I. Stom, S. Goel, B. Xie, Biocathode of microbial fuel cells based on nitrate-reducing strains of Pseudomonas aeruginosa, IOP Conf. Ser. Earth Environ. Sci. 408 (1) (2020), https://doi.org/10.1088/1755-1315/408/1/012084.

[28] Q. Deng, et al., Performance and functional microbial communities of denitrification process of a novel MFC-granular sludge coupling system, Bioresour. Technol. 306 (January) (2020) 123173, https://doi.org/10.1016/j.biortech.2020.123173.

[29] G. Antonopoulou, I. Ntaikou, C. Pastore, L. di Bitonto, S. Bebelis, G. Lyberatos, An overall perspective for the energetic valorization of household food waste using microbial fuel cell technology of its extract, coupled with anaerobic digestion of the solid residue, Appl. Energy 242 (May 2019) 1064–1073, https://doi.org/10.1016/j.apenergy.2019.03.082.

[30] M.M. Mian, G. Liu, B. Fu, Conversion of Sewage Sludge into Environmental Catalyst and Microbial Fuel Cell Electrode Material: A Review, Elsevier B.V., May 20, 2019, https://doi.org/10.1016/j.scitotenv.2019.02.200.

[31] S. Venkata Mohan, G. Mohanakrishna, P.N. Sarma, Composite vegetable waste as renewable resource for bioelectricity generation through non-catalyzed open-air cathode microbial fuel cell, Bioresour. Technol. 101 (3) (Feb. 2010) 970–976, https://doi.org/10.1016/j.biortech.2009.09.005.

[32] M.V. Vilariño, C. Franco, C. Quarrington, Food Loss and Waste Reduction as an Integral Part of a Circular Economy, Frontiers Media S.A, May 17, 2017, https://doi.org/10.3389/fenvs.2017.00021.

[33] M. Kobya, H. Hiz, E. Senturk, C. Aydiner, E. Demirbas, Treatment of potato chips manufacturing wastewater by electrocoagulation, Desalination 190 (1–3) (Apr. 2006) 201–211, https://doi.org/10.1016/j.desal.2005.10.006.

[34] J.J. Fornero, M. Rosenbaum, L.T. Angenent, Electric Power Generation from Municipal, Food, and Animal Wastewaters Using Microbial Fuel Cells, Apr. 2010, https://doi.org/10.1002/elan.200980011.

[35] M.I. Din, M. Iqbal, Z. Hussain, R. Khalid, Bioelectricity generation from waste potatoes using single chambered microbial fuel cell, Energy Sources, Part A Recover. Util. Environ. Eff. 00 (00) (2020) 1–11, https://doi.org/10.1080/15567036.2020.1797944.

[36] R. Rossi, G. Baek, P.E. Saikaly, B.E. Logan, Continuous flow microbial flow cell with an anion exchange membrane for treating low conductivity and poorly buffered wastewater, ACS Sustain. Chem. Eng. 9 (7) (Feb. 2021) 2946–2954, https://doi.org/10.1021/acssuschemeng.0c09144.

[37] S.E. Oh, B.E. Logan, Proton exchange membrane and electrode surface areas as factors that affect power generation in microbial fuel cells, Appl. Microbiol. Biotechnol. 70 (2) (Mar. 2006) 162–169, https://doi.org/10.1007/s00253-005-0066-y.

[38] L. Zhuang, S. Zhou, Y. Yuan, M. Liu, Y. Wang, A novel bioelectro-Fenton system for coupling anodic COD removal with cathodic dye degradation, Chem. Eng. J. 163 (1–2) (Sep. 2010) 160–163, https://doi.org/10.1016/j.cej.2010.07.039.

[39] M. Rahimnejad, A.A. Ghoreyshi, G. Najafpour, T. Jafary, Power generation from organic substrate in batch and continuous flow microbial fuel cell operations, Appl. Energy 88 (11) (2011) 3999–4004, https://doi.org/10.1016/j.apenergy.2011.04.017.

[40] Y. Dessie, S. Tadesse, Y. Adimasu, Improving the performance of graphite anode in a Microbial Fuel Cell via PANI encapsulated α-MnO2 composite modification for efficient power generation and methyl red removal, Chem. Eng. J. Adv. 10 (May 2022), https://doi.org/10.1016/j.ceja.2022.100283.

[41] H. Luo, et al., Electricity generation in a microbial fuel cell using yogurt wastewater under alkaline conditions, RSC Adv. 7 (52) (2017) 32826–32832, https://doi.org/10.1039/c7ra06131e.

[42] J. Myung, P.E. Saikaly, B.E. Logan, A Two-Staged System to Generate Electricity in Microbial Fuel Cells Using Methane, 2018.

[43] Y. Fan, H. Hu, H. Liu, Response to comment on 'sustainable power generation in microbial fuel cells using bicarbonate buffer and proton transfer mechanisms, Environ. Sci. Technol. 42 (16) (2008) 6306, https://doi.org/10.1021/es801335c.

[44] E. Zhang, W. Zhai, Y. Luo, K. Scott, X. Wang, G. Diao, Acclimatization of microbial consortia to alkaline conditions and enhanced electricity generation, Bioresour. Technol. 211 (2016) 736–742, https://doi.org/10.1016/j.biortech.2016.03.115.

[45] M. Mahdi Mardanpour, M. Nasr Esfahany, T. Behzad, R. Sedaqatvand, Single chamber microbial fuel cell with spiral anode for dairy wastewater treatment, Biosens. Bioelectron. 38 (1) (Oct. 2012) 264–269, https://doi.org/10.1016/j.bios.2012.05.046.

[46] M. Jafari, A.H. Mansoorian, Hhvi, A.J. Jafari, N. Khanjani, Evaluation of dairy industry wastewater treatment and simultaneous bioelectricity generation in a catalyst-less and mediator-less membrane microbial fuel cell, J. Saudi Chem. Soc. 20 (1) (2016) 88–100, https://doi.org/10.1016/j.jscs.2014.08.002.

[47] D. Pocaznoi, B. Erable, M.L. Delia, A. Bergel, Ultra microelectrodes increase the current density provided by electroactive biofilms by improving their electron transport ability, Energy Environ. Sci. 5 (1) (Jan. 2012) 5287–5296, https://doi.org/10.1039/c1ee01469b.

[48] M. Verma, V. Mishra, Bioelectricity generation by microbial degradation of banana peel waste biomass in a dual-chamber S. cerevisiae-based microbial fuel cell, Biomass Bioenergy 168 (June 2022) (2023) 106677, https://doi.org/10.1016/j.biombioe.2022.106677.

[49] C. Li, K. Yi, S. Hu, W. Yang, Cathodic biofouling control by microbial separators in air-breathing microbial fuel cells, Environ. Sci. Ecotechnology 15 (Jul) (2023), https://doi.org/10.1016/j.ese.2023.100251.
[50] M. Behera, M.M. Ghangrekar, Performance of microbial fuel cell in response to change in sludge loading rate at different anodic feed pH, Bioresour. Technol. 100 (21) (Nov. 2009) 5114–5121, https://doi.org/10.1016/j.biortech.2009.05.020.
[51] N. Rashid, Y.F. Cui, S.U.R. Muhammad, J.I. Han, Enhanced electricity generation by using algae biomass and activated sludge in microbial fuel cell, Sci. Total Environ. 456–457 (2013) 91–94, https://doi.org/10.1016/j.scitotenv.2013.03.067.
[52] Z. Li, R. Haynes, E. Sato, M.S. Shields, Y. Fujita, C. Sato, Microbial community analysis of a single chamber microbial fuel cell using potato wastewater, Water Environ. Res. 86 (4) (Apr. 2014) 324–330, https://doi.org/10.2175/106143013x13751480308641.
[53] H.J. Mansoorian, A.H. Mahvi, A.J. Jafari, M.M. Amin, A. Rajabizadeh, N. Khanjani, Bioelectricity generation using two chamber microbial fuel cell treating wastewater from food processing, Enzyme Microb. Technol. 52 (6–7) (2013) 352–357, https://doi.org/10.1016/j.enzmictec.2013.03.004.
[54] G.S. Jadhav, M.M. Ghangrekar, Performance of microbial fuel cell subjected to variation in pH, temperature, external load and substrate concentration, Bioresour. Technol. 100 (2) (2009) 717–723, https://doi.org/10.1016/j.biortech.2008.07.041.
[55] P. Nouri, G. Najafpour Darzi, Impacts of process parameters optimization on the performance of the annular single chamber microbial fuel cell in wastewater treatment, Eng. Life Sci. 17 (5) (2017) 545–551, https://doi.org/10.1002/elsc.201600173.
[56] Q. Jia, L. Wei, H. Han, J. Shen, Factors that influence the performance of two-chamber microbial fuel cell, Int. J. Hydrogen Energy 39 (25) (2014) 13687–13693, https://doi.org/10.1016/j.ijhydene.2014.04.023.
[57] L. Zhuang, S. Zhou, Y. Li, Y. Yuan, Enhanced performance of air-cathode two-chamber microbial fuel cells with high-pH anode and low-pH cathode, Bioresour. Technol. 101 (10) (May 2010) 3514–3519, https://doi.org/10.1016/j.biortech.2009.12.105.
[58] Z. Ren, T.E. Ward, J.M. Regan, Electricity production from cellulose in a microbial fuel cell using a defined binary culture, Environ. Sci. Technol. 41 (13) (2007) 4781–4786, https://doi.org/10.1021/es070577h.
[59] B. Min, Ó.B. Román, I. Angelidaki, Importance of temperature and anodic medium composition on microbial fuel cell (MFC) performance, Biotechnol. Lett. 30 (7) (2008) 1213–1218, https://doi.org/10.1007/s10529-008-9687-4.
[60] H. Liu, S. Cheng, B.E. Logan, Power generation in fed-batch microbial fuel cells as a function of ionic strength, temperature, and reactor configuration, Environ. Sci. Technol. 39 (14) (2005) 5488–5493, https://doi.org/10.1021/es050316c.
[61] Y. Feng, X. Wang, B.E. Logan, H. Lee, Brewery wastewater treatment using air-cathode microbial fuel cells, Appl. Microbiol. Biotechnol. 78 (5) (2008) 873–880, https://doi.org/10.1007/s00253-008-1360-2.
[62] A. Larrosa-Guerrero, K. Scott, I.M. Head, F. Mateo, A. Ginesta, C. Godinez, Effect of temperature on the performance of microbial fuel cells, Fuel 89 (12) (2010) 3985–3994, https://doi.org/10.1016/j.fuel.2010.06.025.
[63] L.H. Li, Y.M. Sun, Z.H. Yuan, X.Y. Kong, Y. Li, Effect of temperature change on power generation of microbial fuel cell, Environ. Technol. 34 (13–14) (2013) 1929–1934, https://doi.org/10.1080/09593330.2013.828101.
[64] H. Moon, I.S. Chang, B.H. Kim, Continuous electricity production from artificial wastewater using a mediator-less microbial fuel cell, Bioresour. Technol. 97 (4) (Mar. 2006) 621–627, https://doi.org/10.1016/j.biortech.2005.03.027.